frontiers | Frontiers in Earth Science

TYPE Original Research
PUBLISHED 19 March 2025
DOI 10.3389/feart.2025.1554812

OPEN ACCESS

EDITED BY
Yifei Sun,
Taiyuan University of Technology, China

REVIEWED BY
Yue Yao,
Jiangsu Open University, China
Liu Zhenghao,
Tongji University, China

*CORRESPONDENCE
Wenwei Li,
✉ 180804010002@hhu.edu.cn

RECEIVED 03 January 2025
ACCEPTED 11 February 2025
PUBLISHED 19 March 2025

CITATION
Yan Q, Peng B, Li W, Wang B, Zuo J, Lv G and Wang T (2025) Low-carbon stabilization of expansive soils using cement kiln dust and calcium carbide slag: mechanisms and performance.
Front. Earth Sci. 13:1554812.
doi: 10.3389/feart.2025.1554812

Low-carbon stabilization of expansive soils using cement kiln dust and calcium carbide slag: mechanisms and performance

Qiangzhen Yan[1], Bo Peng[1], Wenwei Li[2,3]*, Baotian Wang[4], Jinyu Zuo[4], Guangdong Lv[5] and Tongzhang Wang[6]

[1]Environmental Branch, Gansu Institute of Engineering Geology, Lanzhou, China, [2]School of Civil Engineering, Shandong University, Jinan, China, [3]Jiangsu Hanjian Group Co., Ltd., Yangzhou, China, [4]Laboratory of Ministry of Education for Geomechanics and Embankment Engineering, Hohai University, Nanjing, China, [5]Water Conservancy Civil Engineering College, Tibet Agriculture and Animal Husbandry University, Nyingchi, China, [6]Jiangsu Hehai Engineering Technology Co., Ltd., Nanjing, China

In response to the environmental challenges posed by conventional expansive soil stabilization methods, this study investigates the low-carbon potential of industrial by-products—cement kiln dust (CKD) and calcium carbide slag (CCS)—as sustainable stabilizers. A comprehensive series of laboratory tests, including compaction tests, free swelling rate measurements, unconfined compressive strength (UCS) evaluations, and scanning electron microscopy (SEM) analyses, were conducted on expansive soil samples treated with varying dosages in both single and binary formulations. The results indicate that the binary system significantly outperforms individual stabilizers; for example, a formulation containing 10% CKD and 9% CCS achieved a maximum dry density of 1.64 g/cm^3, reduced the free swelling rate to 22.7% at 28 days, and reached a UCS of 371.3 kPa. SEM analysis further revealed that the enhanced performance is due to the synergistic formation of hydration products—namely calcium silicate hydrate (C-S-H) and calcium aluminate hydrate (C-A-H)—which effectively fill interparticle voids and reinforce soil structure. These findings demonstrate that the dual mechanism, combining rapid early-stage hydration from CCS with sustained long-term strength development from CKD, offers a cost-effective and environmentally sustainable alternative to traditional stabilizers for expansive soils.

KEYWORDS

expansive soil, cement kiln dust, calcium carbide slag, soil stabilization, microstructural analysis, sustainable construction materials

1 Introduction

Soil instability poses critical challenges to geotechnical engineering, manifesting in diverse forms such as slope failures (Song et al., 2024), foundation subsidence (Shan et al., 2022), and vibration-induced structural damage (Liu et al., 2024). Among these issues, expansive soils represent a particularly problematic category of geomaterials due to their propensity for significant volumetric changes in response to moisture variations. These volumetric fluctuations can lead to severe infrastructure distress, including

cracking, uneven settling, and reduced service life (Abbas et al., 2023; Ye et al., 2023; Laporte et al., 2023; Sarker et al., 2023). In Jiangsu Province, China, expansive soils underlie a range of important slope engineering projects, where repeated slope instabilities pose severe risks to transportation corridors, embankments, and other critical structures. Historically, civil engineers have relied on cement and lime as primary stabilizing agents to mitigate these deleterious volume-change effects (Wei et al., 2023; Zada et al., 2023). While undeniably effective in controlling soil swelling and improving load-bearing capacity, these conventional stabilizers pose critical challenges in the modern era due to their carbon-intensive production processes (Syed et al., 2023; Zhang et al., 2023). Their reliance on substantial energy inputs and fossil fuel combustion has generated mounting concern from environmental stakeholders, regulators, and project owners seeking to align construction operations with contemporary sustainability directives. Consequently, identifying low-carbon alternatives that retain or exceed the efficacy of traditional methods has emerged as a central focus in soil improvement science, reflecting the broader movement toward climate-responsive infrastructure development (Chen et al., 2021; Miraki et al., 2022). In this context, the search for innovative soil stabilization methodologies that reduce carbon emissions while maintaining or enhancing performance has become increasingly urgent.

In response to the escalating challenges posed by global climate change, the pursuit of low-carbon and environmentally sustainable construction materials has become a pressing objective within the civil engineering domain (Fatima et al., 2023; Hassan et al., 2023). Indeed, the cement industry alone is estimated to contribute approximately 7%–8% of global CO_2 emissions, with the production of one tonne of ordinary Portland cement typically releasing about 0.8–0.9 tonnes of CO_2 (Habert et al., 2020). Lime production also involves energy-intensive calcination processes that contribute significantly to greenhouse gas emissions. This urgent imperative arises from the need to reduce overall carbon output, conserve natural resources, and promote circular economy practices. Accordingly, the development and deployment of novel soil improvement strategies that embrace low-carbon stabilizers have gained significant traction in geotechnical research and practice. In particular, employing industrial by-products for soil stabilization can simultaneously meet performance requirements for strength and durability while minimizing environmental footprints. Moreover, the integration of such waste-derived binders into soil improvement processes not only enhances mechanical properties but also contributes to reduced raw material consumption, thereby enabling more responsible use of natural resources. Consequently, this approach to soil stabilization represents a vital step forward in realizing sustainable resource management practices at both local and global scales (Dang et al., 2021; Barman and Dash, 2022; Tiwari et al., 2021).

Within this conceptual framework, the utilization of industrial waste products as alternative stabilizers has garnered growing attention, driven by the dual imperatives of enhancing performance and promoting environmental sustainability. Generally, these waste-derived materials contribute to soil stabilization through one or more primary mechanisms: pozzolanic reactions (Zheng et al., 2023), cementitious binding (Al-Adhadh et al., 2024), and/or alkaline activation (Syed et al., 2022). By leveraging such mechanisms, researchers not only address the swelling and strength limitations of expansive soils but also advance circular economy principles by repurposing by-products otherwise destined for landfills.

Among these materials, fly ash stands out for its prominent pozzolanic properties. As a voluminous by-product of coal combustion, fly ash contains substantial quantities of silica and alumina that can react with calcium in soil or other binders to form cementitious hydrates, thereby refining the pore structure and improving load-bearing capacity (Mahedi et al., 2020; Chen et al., 2022). In contrast, steel slag (Wu et al., 2021) and ground granulated blast furnace slag (GGBS) (Al-Saedi and Sabbar, 2024; Zhao et al., 2023) exhibit both latent hydraulic and pozzolanic characteristics: they can harden in the presence of water and/or supplementary alkalis, thus enhancing soil stiffness and mitigating volumetric instability (Muthukkumaran and Anusudha, 2020; Mustafayeva et al., 2024). Meanwhile, materials with inherently high calcium oxide (CaO) content—such as cement kiln dust (CKD) and calcium carbide slag (CCS)—contribute significantly to alkaline activation. By elevating the soil's pH, these high-lime residues foster flocculation of clay particles and promote the formation of additional hydration products. CKD, collected as fine particulates during cement production, is rich in silica, alumina, and CaO, enabling robust pozzolanic interactions and the generation of calcium silicate hydrates (Wei et al., 2023; Attah et al., 2021; Almuaythir and Abbas, 2023; Al-Bakri et al., 2022). CCS, derived from acetylene production, also contains elevated levels of CaO, creating conditions conducive to accelerated formation of cementitious compounds (Chu et al., 2023; Gong et al., 2022; Wang et al., 2024).

Despite the proven utility of each waste material in isolation, research exploring combined or binary stabilizer formulations—particularly involving CKD and CCS—remains relatively limited. Consequently, deeper insights into optimal dosage strategies, specific reaction pathways, and attendant improvements in soil performance are needed. The present study therefore undertakes a comprehensive investigation of expansive soil stabilization using CKD and CCS, both individually and in combination, to elucidate these stabilization mechanisms more fully. Through a multi-pronged experimental approach encompassing compaction tests, free swelling rate assessments, unconfined compressive strength (UCS) measurements, and scanning electron microscopy (SEM) analyses, this study aims to illuminate how best to harness the synergistic potential of CKD and CCS for expansive soil improvement. The findings not only provide robust technical guidance on deploying these by-products as low-carbon stabilizers but also underscore the broader sustainability benefits of industrial waste reutilization in geotechnical applications.

2 Materials and methods

2.1 Materials

The primary experimental materials used in this study include expansive soil, cement kiln dust, and calcium carbide slag (as shown in Figure 1), all of which were collected and prepared

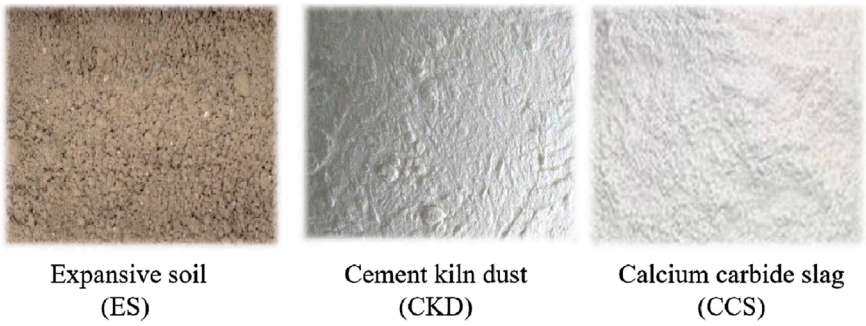

FIGURE 1
Materials used in this study.

TABLE 1 Basic properties of expansive soil used.

Free expansion rate δ_{ef} (%)	Natural dry density p (g/cm^3)	Optimum moisture content ω_{op} (%)	Maximum dry density ρ_d (g/cm^3)	Plastic limit ω_L (%)	Liquid limit ω_P (%)	Plasticity index IL (%)	Specific gravity Gs
52	1.42	18.9	1.55	23.6	51.2	27.6	2.72

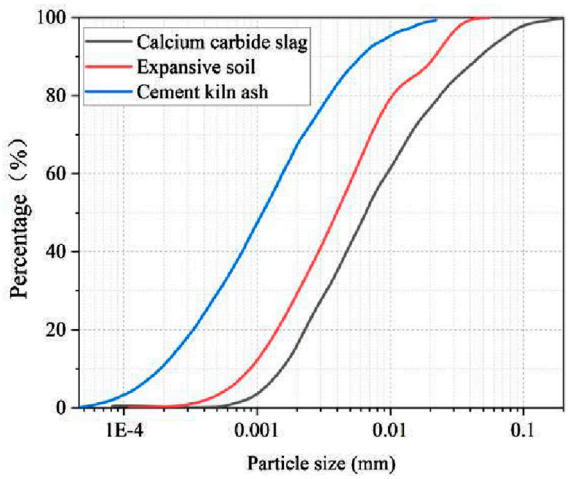

FIGURE 2
The gradation curves for cement kiln dust, calcium carbide slag, and expansive soil.

TABLE 2 Chemical compositions of the cement kiln ash.

Chemical composition	Content/%
Cao	51.95
SiO_2(%)	21.86
Al_2O_3(%)	4.23
Fe_2O_3(%)	4.76
MgO (%)	3.20
Others (%)	14

under strictly controlled conditions. The expansive soil used in this study was collected from a landslide in Gaochun District, Nanjing, Jiangsu Province, China. The soil is regarded as waste soil in the local engineering project due to the high uncertainty and hazard. The basic properties were tested by field density test, compaction test, liquid-plastic limit test and specific gravity test according to the "Standard for Geotechnical Testing Methods" (GB/T50123-2019) (Ministry of Construction P.R.China, 2019). The values obtained were summarized in Table 1, and the gradation curve was shown in Figure 2.

Cement kiln dust (CKD) is an industrial waste product derived from the cement production process, with primary chemical components including calcium oxide (CaO), silicon dioxide (SiO_2), and aluminum oxide (Al_2O_3), as well as small amounts of alkali oxides and sulfates. Cement kiln dust exhibits pozzolanic activity, with fine particles that can fill soil pores, thus improving the soil structure. The cement kiln dust used for the experiment was sourced from a cement plant in Henan Province, with its main components and parameters shown in Table 2.

Calcium carbide slag (CCS) is a by-product generated during the production of acetylene, primarily composed of calcium hydroxide ($Ca(OH)_2$), and has a strong alkalinity. The calcium carbide slag can undergo a hydration reaction with silicates and aluminates in the soil, producing calcium silicate hydrate (C-S-H) and calcium aluminate hydrate (C-A-H), thus improving the strength and stability of the soil. The calcium carbide slag used in the experiment

TABLE 3 Details of the stabilized soil samples.

Experiment number	Group	Cement kiln dust content/%	Calcium carbide slag content/%
CG-0/0[a]	Control group (CG)	0	0
BSS-5/6[b]	Binary Stabilizer System (BSS)	5	6
BSS-5/9		5	9
BSS-5/12		5	12
BSS-10/6		10	6
BSS-10/9		10	9
BSS-10/12		10	12
BSS-15/6		15	6
BSS-15/9		15	9
BSS-15/12		15	12
SSS-K5[c]	Single Stabilizer System (SSS)	5	0
SSS-K10		10	0
SSS-K15		15	0
SSS-C6[d]		0	6
SSS-C9		0	9
SSS-C12		0	12

[a]CG-0/0 indicates the Control Group with 0% CKD, and 0% CCS.
[b]BSS-x/y refers to the Binary Stabilizer System, where x% CKD, is combined with y% CCS (e.g., BSS-5/6 has 5% CKD +6% CCS).
[c]SSS-Kx denotes the Single Stabilizer System with only CKD, at x% (e.g., SSS-K10, has 10% CKD, and 0% CCS).
[d]SSS-Cy denotes the Single Stabilizer System with only CCS, at y% (e.g., SSS-C9, has 0% CKD, and 9% CCS).

was obtained from a chemical plant in Hunan Province, with a $Ca(OH)_2$ content of 93.00%.

2.2 Experiment methods

2.2.1 Experimental design

This investigation systematically evaluates the modification mechanisms of expansive soil matrices by utilizing cement kiln dust (CKD) and calcium carbide slag (CCS) as stabilizing agents. To facilitate clear comparisons across different formulations, the experimental program is organized into four main categories, as summarized in Table 3: (1) a control group with no stabilizer addition (CG-0/0), (2) a CKD-only series (SSS-K) at three dosage levels, (3) a CCS-only series (SSS-C) at three dosage levels, and (4) a set of binary stabilizer series (BSS) with combined CKD and CCS additions.

In the CKD-only (SSS-K) series, CKD is incorporated at concentrations of 5%, 10%, and 15%, where hydration reactions facilitate the formation of calcium silicate hydrate (C-S-H) and calcium aluminate hydrate (C-A-H). Similarly, the CCS-only (SSS-C) series includes CCS at concentrations of 6%, 9%, and 12%, wherein its principal constituent, calcium hydroxide (Ca(OH)2), suppresses expansion and enhances strength through reactions with soil minerals. The mono-component stabilizer configurations (i.e., SSS-K and SSS-C) enable a systematic evaluation of individual stabilizer efficacy, whereas the binary stabilizer series (BSS) assesses potential synergistic enhancements to both mechanical properties and dimensional stability when CKD and CCS are used in combination. Establishing CG-0/0 as the control baseline allows quantitative assessment of stabilizer-induced performance improvements.

A multi-parameter experimental methodology—encompassing compaction tests, free swelling rate measurements, unconfined compressive strength (UCS) evaluations, and scanning electron microscopy (SEM) analyses—was adopted to capture both macroscopic and microstructural changes. By comparing different stabilizer dosages and single/binary combinations, this study elucidates the impact of CKD and CCS on critical engineering parameters, such as compressive strength and swelling behavior, thereby informing optimal dosage strategies.

2.2.2 Experimental method

In order to comprehensively evaluate the mechanical properties and swelling characteristics of cement kiln dust and calcium carbide slag-modified expansive soil, this study

conducted several laboratory tests, including compaction tests, unconfined compressive strength tests, free swelling rate tests, and microstructure analysis. The following are the specific methods of each test:

2.2.2.1 Compaction test

In this study, the sample preparation process for expansive soil first requires determining the optimum moisture content and maximum dry density for each dosage through compaction tests. These parameters are essential to ensure the optimal compaction of soil samples during preparation, thereby ensuring the accuracy of the test results. The compaction test was conducted according to the "Standard for Geotechnical Testing Methods" (GB/T50123-2019) (Ministry of Construction P.R.China, 2019), using the heavy compaction method. Samples with different combinations of cement kiln dust and calcium carbide slag contents were compacted in layers to determine the optimum moisture content and maximum dry density for each mix ratio.

2.2.2.2 Free swelling rate test

This study investigated the variations in expansive properties of modified expansive soil through free swelling rate tests, conducted in accordance with the "Standard for Soil Test Methods" (GB/T50123-2019) (Ministry of Construction P.R.China, 2019). Initially, the central portion was extracted from the cured unconfined compression specimens, air-dried, and subsequently pulverized to pass through a 0.5 mm sieve. A 50 g sample was then collected for the swell ratio test. During the experimental procedure, the specimen was placed in a cylindrical vessel with dimensions of 100 mm in height. Deionized water was gradually introduced until the water level was flush with the soil specimen surface. After a 24-h immersion period, the expansion height was measured to calculate the free swelling rate, thereby evaluating the changes in expansive properties of the modified soil. The free swelling rate was calculated using the Equation 1:

$$\text{Free swelling rate} = \left(\Delta H / H_0\right) \times 100\% \quad (1)$$

Where ΔH represents the change in specimen height after swelling, and H_0 denotes the initial height of the specimen.

2.2.2.3 Unconfined compressive strength test

This study evaluated the strength performance of the modified soil using unconfined compressive strength tests, which were conducted according to the "Specifications for Highway Subgrade Testing" (JTG E40-2007) (Ministry of Transport P.R. China, 2007), using a WDW-10E electronic universal testing machine to measure compressive strength. The preparation of the specimens followed the mix design plan, using a static compaction method to form cylindrical specimens with a diameter of 50 mm and a height of 100 mm, with a compaction degree of 96% of the maximum dry density. The molded specimens were sealed and placed in a standard curing chamber, maintained at a temperature of 23°C ± 2°C and a relative humidity of over 95%. The curing periods were set at 7, 14, and 28 days. After the curing period, the specimens were removed from the curing chamber, placed on the testing machine, and loaded at a constant rate of 1 mm/min until failure, with the failure load being recorded.

The unconfined compressive strength (UCS) is calculated by Equation 2:

$$UCS = P/A \quad (2)$$

Where P is the maximum load at failure, and A is the cross-sectional area of the specimen.

2.2.2.4 Microstructural analysis

This research employed Scanning Electron Microscopy (SEM) technology to analyze the microstructure of soil modified with cement kiln dust and calcium carbide slag, aiming to investigate the modification mechanisms. As a high-resolution microscopic imaging technique, SEM can reveal detailed information about particle morphology, pore distribution, and cementitious material formation within the soil matrix, which is crucial for understanding the microstructural and mechanical properties of modified materials. In the experimental procedure, small specimens were first extracted from the failure surface of unconfined compression test samples. These specimens underwent drying treatment followed by gold coating to prevent charging effects during electron beam scanning. Subsequently, observations were conducted using a HITACHI SU8010 high-resolution scanning electron microscope, obtaining three-dimensional morphological and compositional information through secondary electron and backscattered electron imaging. The SEM images clearly illustrated the distribution of cementitious materials between particles, changes in pore structure, and the formation of microscopic connection networks in the modified soil samples.

Through the aforementioned experimental methods, this study systematically analyzed the individual and combined modification effects of cement kiln dust and calcium carbide slag, evaluated their effectiveness in improving the strength and expansive characteristics of expansive soil, and revealed the modification mechanisms from a microscopic perspective.

3 Results and analysis

3.1 Compaction characteristics

Building on the preliminary soil characterizations from Section 2, this subsection analyzes how varying CKD and CCS contents affect the compaction behavior of expansive soils. Figures 3, 4 depict the maximum dry density (MDD) and optimal moisture content (OMC) for each mix ratio, revealing systematic variations in compaction characteristics as cement kiln dust (CKD) and calcium carbide slag (CCS) contents change.

Compared to the control group (MDD = 1.55 g/cm^3, OMC = 18.6%), single-stabilizer systems (SSS) show notable improvements in compaction parameters. Specifically, a 5% CKD addition (SSS-K5) reduces the OMC to 18.2% and increases the MDD to 1.62 g/cm^3, while 6% CCS (SSS-C6) achieves an OMC of 18.3% and an MDD of 1.63 g/cm^3. These enhancements are attributable to reduced free water demand and improved compaction efficiency. The stabilizers occupy voids within the soil matrix and generate cementitious hydration products (e.g., calcium silicate hydrate), effectively refining the pore structure and facilitating densification.

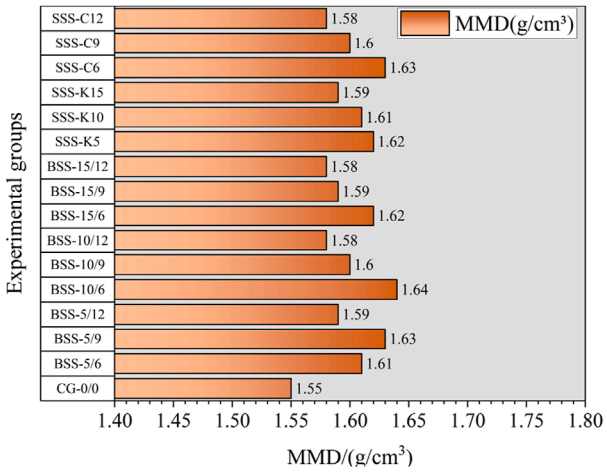

FIGURE 3
Maximum dry density (MMD) for each mix ratio.

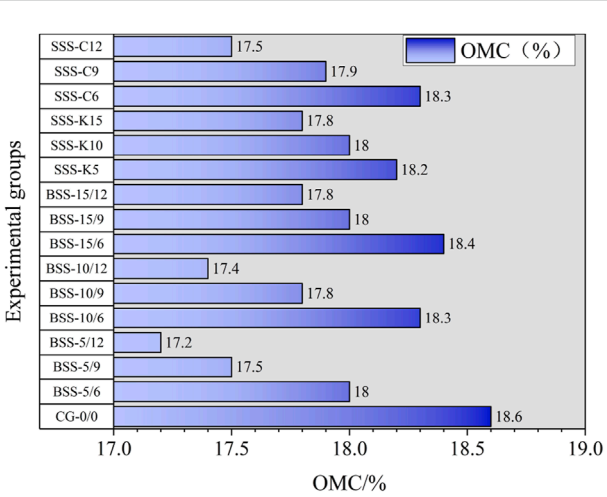

FIGURE 4
Optimal moisture content (OMC) for each mix ratio.

Comparisons between single- (SSS) and binary-stabilizer systems (BSS) illustrate that binary additions generally yield superior compaction performance at intermediate dosage levels. For instance, the BSS-5/9 configuration realizes an OMC of 17.5% and an MDD of 1.63 g/cm^3, a net increase of 0.08 g/cm^3 over the control. This outcome underscores the synergistic effect arising from simultaneously adding CKD and CCS, whereby accelerated hydration kinetics and enhanced void-filling contribute to improved matrix consolidation. Relative to corresponding single-stabilizer mixes (e.g., 5% CKD only or 9% CCS only), the binary formulation exhibits appreciably higher density and reduced moisture demand, demonstrating the robust synergistic mechanisms that underpin BSS performance.

At higher stabilizer concentrations, however, the incremental gains in maximum dry density appear to diminish. Although the BSS-15/12 configuration achieves an OMC of 17.8% and an MDD of 1.58 g/cm^3, it does not surpass certain intermediate formulations—such as BSS-10/6, which reaches an MDD of 1.64 g/cm^3. These findings suggest that excessive stabilizer content may impede uniform inter-particle distribution and introduce saturation-like effects that inhibit additional compaction benefits. In contrast, intermediate-dosage configurations (e.g., BSS-10/6) strike a favorable balance between material input and achievable densification, thereby offering an optimal cost–performance ratio. Collectively, these observations highlight the importance of targeted CKD–CCS proportions in achieving both enhanced compaction and economic efficiency when stabilizing expansive soils.

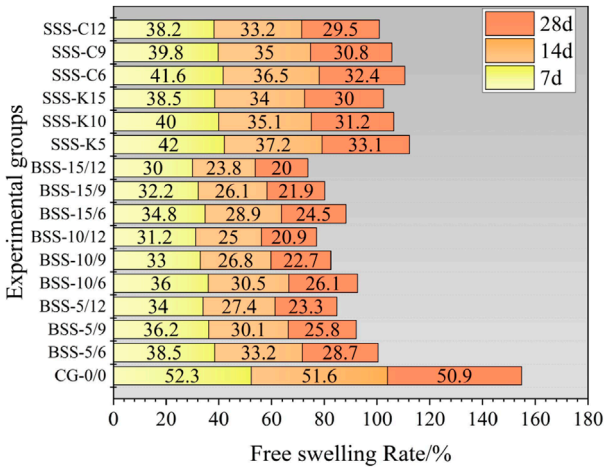

FIGURE 5
Changes in free swelling rate for different stabilized samples.

3.2 Free swelling rate analysis

Following the compaction analysis in Section 3.1, this subsection focuses on the influence of different CKD and CCS dosages on the free swell behavior of expansive soils. Figure 5 delineates the temporal evolution of free swelling rate parameters across diverse stabilizer configurations throughout prescribed curing time of 7, 14, and 28 days. Empirical analysis demonstrates that progressive elevation in stabilizer concentrations, specifically cement kiln dust (CKD) and calcium carbide slag (CCS), manifests in substantial attenuation of free swell characteristics in modified expansive soil matrices. Moreover, the binary stabilizer system (BSS) exhibits markedly superior expansiveness suppression efficacy relative to monolithic stabilizer configurations (SSS). Specifically, the BSS-5/6 configuration yielded an initial free swelling rate of 38.5% at 7-day curing duration, subsequently exhibiting progressive reduction to 28.7% at 28-day maturation, representing a substantial diminution of 22.2 percentage points relative to control specimens (CG-0/0). Further optimization through elevated CCS incorporation, as manifested in the BSS-5/12 configuration, demonstrated enhanced performance characteristics, yielding an initial free swelling rate of 34.0% at 7-day curing duration, followed by significant reduction to 23.3% at 28-day maturation, corresponding to a marked decrease of 27.6 percentage points comparative to control specimens.

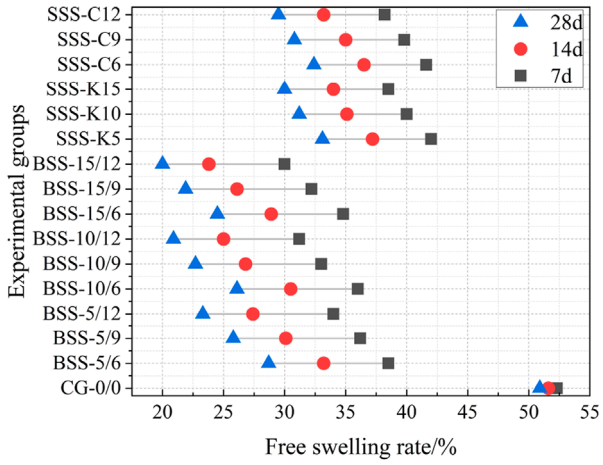

FIGURE 6
Changes in free swelling rate with curing times.

The BSS configuration manifests dual physicochemical functionality through C-S-H and C-A-H generation, facilitating concurrent void space occupation and matrix stability enhancement, thereby achieving significant expansiveness suppression. The BSS-10/9 configuration demonstrated superior performance characteristics, exhibiting an expansion coefficient reduction to 22.7% at 28-day curing duration, representing decrements of 10.3 and 28.2 percentage points relative to 7-day measurements and CG-0/0 specimens, respectively. In contrast, the SSS configurations exhibited marginally diminished efficacy, with SSS-K10 and SSS-C9 yielding expansion coefficients of 31.2% and 30.8%, respectively, at 28-day maturation. Despite demonstrable improvements through single stabilizer incorporation, the singular physicochemical mechanisms manifested constrained effectiveness, failing to achieve the synergistic inhibitory phenomena characteristic of binary systems.

Figure 6 shows the changes in free swelling rate with curing times. The temporal evolution of free swell characteristics exhibits significant attenuation concurrent with curing duration extension, particularly pronounced in BSS configurations where expansion coefficient reduction demonstrates progressive enhancement. Initial modifications manifest at 7-day curing duration, exemplified by BSS-10/9 configuration yielding an expansion coefficient of 33.0%, corresponding to a 19.3 percentage point reduction relative to CG-0/0 specimens. Subsequent maturation to 14-day duration facilitates enhanced pore structure modification through progressive hydration product development, yielding further reduction to 26.8%. Terminal measurements at 28-day curing duration demonstrate optimized stabilization of reaction products, manifesting in an expansion coefficient of 22.7%, representing a substantial decrement of 10.3 percentage points relative to 7-day measurements.

The modification efficacy of BSS configurations exhibits progressive enhancement concurrent with curing duration extension. Specifically, the BSS-15/12 configuration demonstrates significant performance optimization at 14-day maturation, manifesting a free swelling rate reduction to 20.0%, corresponding to a 10 percentage point decrement relative to 7-day measurements, thereby validating the enhanced stabilizer reactivity under prolonged curing conditions. Furthermore, elevated BSS configurations, exemplified by BSS-15/12, exhibit superior expansiveness suppression, achieving a 32.3 percentage point reduction at 28-day maturation relative to SSS configurations.

The synergistic incorporation of stabilizing agents in BSS configurations demonstrates markedly enhanced expansiveness suppression efficacy comparative to SSS configurations, particularly pronounced at intermediate to elevated dosages under extended curing durations. Progressive matrix densification and stability enhancement manifest through systematic pore structure modification via hydration product evolution. While SSS configurations demonstrate measurable expansiveness suppression, their limited physicochemical modification mechanisms yield comparatively diminished efficacy. Empirical analysis indicates that BSS-10/9 configuration achieves optimal performance parameters, manifesting an expansion ratio of 22.7% at 28-day maturation, thereby establishing an optimal equilibrium between economic considerations and modification efficacy for practical engineering applications.

3.3 Strength characteristics

This section presents a detailed analysis of unconfined compressive strength (UCS) under varying curing conditions, elucidating how binary stabilizer systems (BSS) exploit potential synergistic interactions between cement kiln dust (CKD) and calcium carbide slag (CCS) to offer insights into optimal dosage strategies for expansive soil stabilization. Figure 7 shows the changes in UCS with different curing times for different stabilized samples. Within the binary stabilizer matrix, the mechanistic characteristics and performance parameters of CCS and CKD exhibit distinctive temporal variations across curing durations. Empirical analysis elucidates that CCS functions primarily as an activation agent, wherein incremental dosage elevation manifests in accelerated early-stage strength development. The SSS-C series demonstrates systematic strength enhancement correlating with concentration gradients, specifically yielding 7-day strength parameters of 111.8 kPa, 129.2 kPa, and 141.3 kPa for SSS-C6, SSS-C9, and SSS-C12 configurations, respectively. This phenomenon correlates with the enhanced reactivity of CaO components within CCS matrices during soil modification processes. The formation of ettringite, C-S-H gel, and associated hydration products facilitates concurrent enhancement of initial bonding strength and significant attenuation of plasticity and shrinkage characteristics in expansive soil matrices. While this reaction mechanism demonstrates superior early-stage activation efficacy, the long-term strength development contribution exhibits limitations, exemplified by the SSS-C12 configuration achieving merely 171.8 kPa at 28-day maturation. This temporal evolution pattern indicates stabilization of CCS reactivity in terminal stages, with primary efficacy manifesting in early-stage strength enhancement mechanisms.

In contrast to CCS behavior, CKD exhibits progressive strength enhancement characteristics, particularly pronounced during terminal curing phases. Empirical data demonstrates systematic strength optimization correlating with elevated CKD

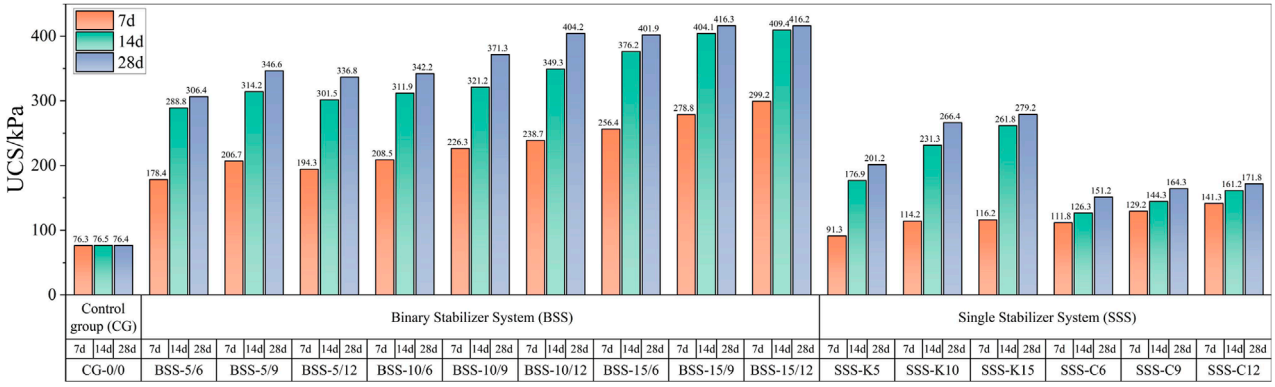

FIGURE 7
Changes in UCS with different curing times for different stabilized samples.

concentrations at 14-day and 28-day maturation intervals. The BSS-10/6 configuration manifests strength parameters of 208.5 kPa, 311.9 kPa, and 342.2 kPa at 7-day, 14-day, and 28-day intervals, respectively, reflecting the sustained hydration kinetics of CKD components. This phenomenon correlates with secondary hydration mechanisms of free calcium oxide, silicates, and aluminates, facilitating progressive matrix densification through C-S-H gel and ettringite formation.

For CKD concentrations ≤10%, optimal strength enhancement manifests in configurations approximating unity CKD:CCS ratios, effectively leveraging early-stage CCS activation concurrent with terminal-stage CKD strength development. The BSS-10/9 and BSS-10/12 configuration exemplifies this optimization. BSS-10/9 yielding progressive strength evolution of 226.3 kPa, 321.2 kPa, and 371.3 kPa across respective curing intervals. CKD concentrations exceeding 10% manifest primarily in early-stage strength enhancement with constrained terminal-stage optimization. The BSS-15/6 configuration yields 256.4 kPa at 7-day maturation, substantially exceeding BSS-10/6 (208.5 kPa); however, terminal strength parameters (401.9 kPa versus 342.2 kPa) demonstrate limited incremental benefit. This phenomenon correlates with accelerated early-stage hydration kinetics at elevated CKD concentrations, culminating in reaction saturation during terminal phases due to comprehensive pore structure modification through C-S-H and ettringite formation.

To systematically evaluate the synergistic efficacy of binary CKD-CCS configurations on expansive soil compressive strength characteristics, this investigation introduces a novel quantitative parameter: the Synergistic Enhancement Factor (SEF). This metric facilitates comprehensive analysis of performance parameters across diverse binary configurations throughout prescribed curing durations, enabling quantitative assessment of BSS efficacy relative to corresponding SSS configurations. The mathematical formulation for SEF determination is expressed as Equation 3:

$$SEF = \Delta\sigma_{BBS} / \Delta\sigma_{SSS-K} + \Delta\sigma_{SSS-C} \quad (3)$$

where:

$\Delta\sigma_{BBS}$ (Combined Strength Increase). This term represents the net improvement in unconfined compressive strength (UCS) realized by the binary stabilizer system (i.e., CKD + CCS used together) compared to the untreated control sample. Physically, it embodies the total effect of both stabilizers acting in tandem, including any additional hydration products or enhanced particle bonding resulting specifically from the interaction of CKD and CCS within the soil matrix.

$\Delta\sigma_{SSS-K}$ (CKD-Only Strength Increase). This parameter captures the individual contribution of cement kiln dust (CKD) as if it were used alone at the same or comparable dosage. In other words, it is the UCS gain relative to the control group when only CKD is applied, reflecting phenomena such as pozzolanic reactions, C-S-H gel formation, and pore structure refinement attributable solely to CKD.

$\Delta\sigma_{SSS-C}$ (CCS-Only Strength Increase). Analogous to ΔSSS-K, this term indicates how much calcium carbide slag (CCS) alone improves the UCS. Its physical significance lies in the early-stage activation potential of CCS, driven by its $Ca(OH)_2$ or CaO content, and the resultant hydration products that form independently of CKD.

A broader comparative examination of SEF trends, (as shown in Figure 8), taking into account both performance and cost-effectiveness, strengthens the conclusion regarding optimal CKD–CCS formulations. Within the lower-CKD category (CKD ≤10%), BSS-5/6 maintains a notable advantage in early-age strength gain, as evidenced by its SEF peak of 2.02 at 7 days—a value exceeding that of BSS-5/9 and BSS-5/12—and remains competitive at 28 days (1.15). Although some higher-CKD formulations—such as BSS-15/6—can achieve even higher SEF values at 7 days, the relatively larger total stabilizer content increases material costs without providing proportionally greater long-term strength improvements. Indeed, while BSS-15/6 achieves a 7-day SEF of 2.39, its 28-day value (1.17) suggests diminishing returns, underscoring its lower cost-effectiveness compared to BSS-5/6 in contexts where both performance and economic factors must be balanced.

In the higher-CKD range (CKD >10%), the SEF trends similarly indicate that BSS-10/9 offers a more attractive balance between short-term efficiency and sustained long-term performance, thereby favorably impacting material costs relative to higher-dosage formulations. For example, BSS-10/9 attains an SEF of 1.65 at 7 days

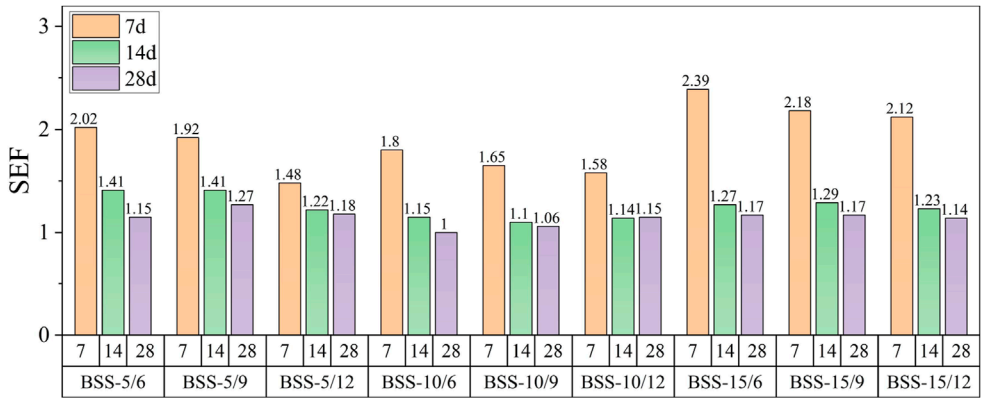

FIGURE 8
Changes in SEF with different curing times for different stabilized samples.

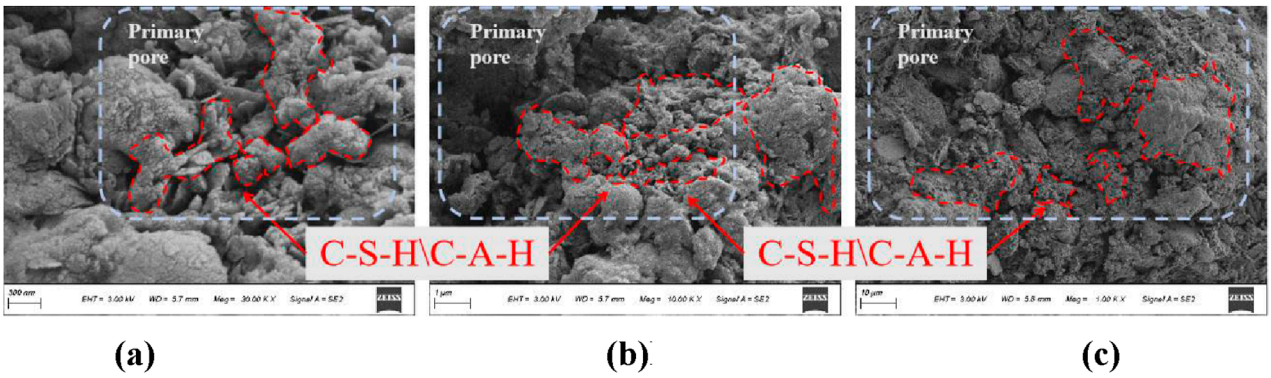

FIGURE 9
The SEM results for BSS-5/6 and BBS-5/10 samples. **(A)** BSS-5/6 (scanning area 1) **(B)** BSS-5/6 (scanning area 2) **(C)** BBS-5/10 (scanning area 1).

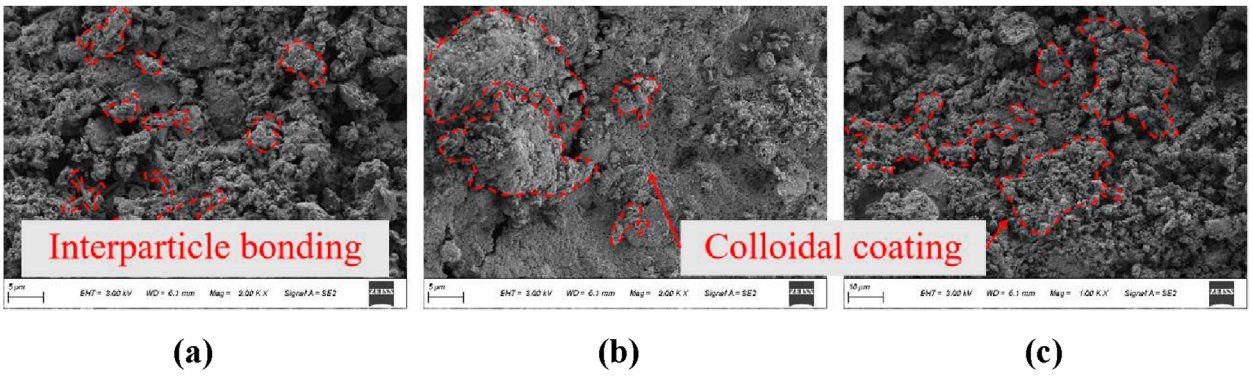

FIGURE 10
The SEM results for BSS-10/9 and BBS-15/12 samples. **(A)** BSS-10/9 (scanning area 1) **(B)** BSS-10/9 (scanning area 1) **(C)** BBS-15/12 (scanning area 2).

and 1.10 at 14 days, effectively balancing early and terminal strength enhancement. By contrast, configurations such as BSS-15/6, despite their high early SEF, exhibit reduced performance gains at extended curing intervals and elevate stabilizer dosage requirements, leading to heightened material expenditures with no commensurate increase in long-term strength. Consequently, BSS-10/9 emerges as the most suitable choice in higher-CKD scenarios when cost-effectiveness and consistent strength development over time are prioritized, complementing the lower-CKD optimum (BSS-5/6) for rapid early gains in expansive soil stabilization.

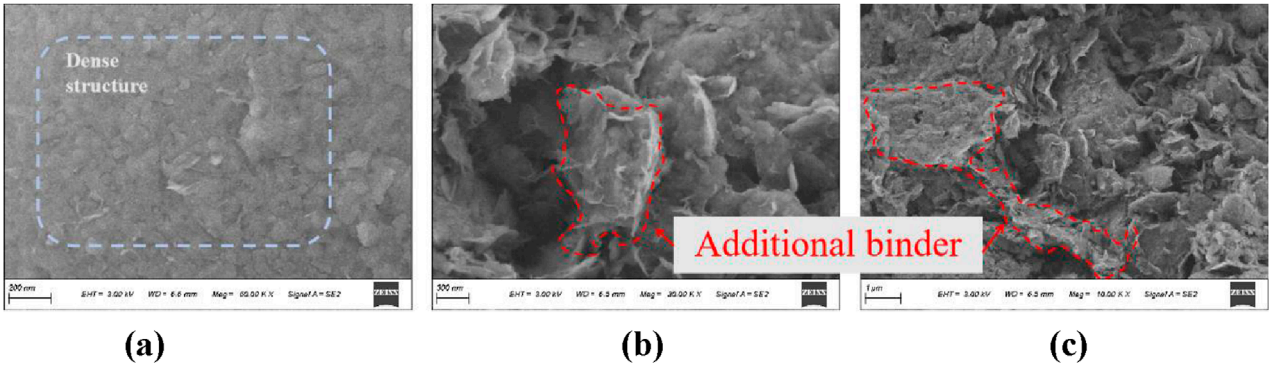

FIGURE 11
The SEM results for high magnification. **(A)** BSS-10/9 (scanning area 3) **(B)** BSS-15/12 (scanning area 1) **(C)** BBS-15/12 (scanning area 2).

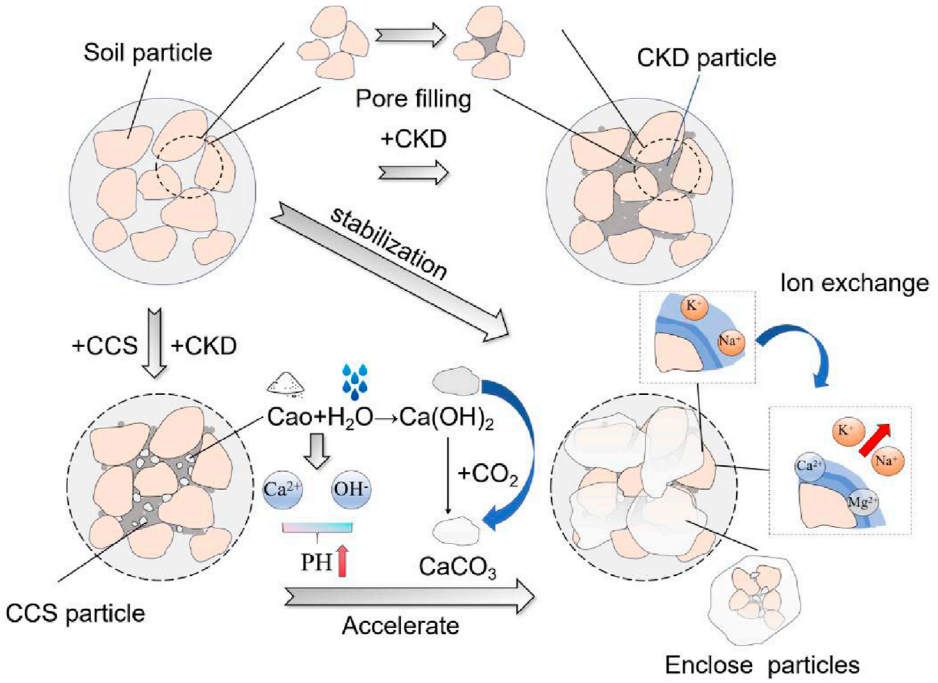

FIGURE 12
The mechanism of stabilizing expansive soil by composite action of CKD and CCS.

3.4 Scanning electron microscopy analysis

As shown in Figure 9, the scanning electron micrographs (SEM) of the cement kiln dust (CKD)–calcium carbide slag (CCS) stabilized expansive soil reveal a pronounced decrease in interparticle voids and the emergence of dense particle clusters. These observations underscore the formation of hydration products, particularly calcium silicate hydrate (C-S-H) and calcium aluminate hydrate (C-A-H), which fill pore spaces and integrate soil grains into cohesive aggregations. Additionally, the fine particles of CKD can physically occupy voids within the soil matrix, reinforcing the densification process alongside the chemical reactions. The resultant microstructure is more compact than that of the untreated control samples, aligning with the elevated maximum dry density (MDD) and reduced free swelling rate recorded in the laboratory tests. By occupying previously unfilled pore spaces, these newly formed cementitious phases effectively limit water infiltration and the attendant volumetric expansion, a phenomenon corroborated by the substantial decrease in free swelling rates observed across various stabilizer configurations.

Figure 10 also illustrate the development of robust interparticle bonding in the binary stabilizer systems, especially at intermediate stabilizer dosages such as BSS-10/6 or BSS-10/9. The synergy between CKD and CCS fosters progressive pozzolanic reactions involving CaO, SiO2, and Al2O3, generating semi-crystalline and amorphous gel phases that coat the soil grains and reinforce

interparticle contact areas. This morphological connectivity reduces stress concentrations under load, thus enhancing unconfined compressive strength (UCS) at both early (7-day) and later (28-day) curing stages. In contrast, higher stabilizer contents can produce a dense, albeit unevenly distributed matrix that may not sustain continued strength gains due to localized agglomeration and diminished reactivity. The BSS-15/12 configuration, for example, appears less effective in the long term despite an initially dense structure, underscoring the importance of balancing stabilizer supply with the soil's reactive capacity.

As shown in Figure 11, Closer examination at high magnification provides further evidence that carefully calibrated CKD–CCS ratios optimize the extent and distribution of hydration products. In intermediate-dosage mixtures, microcracks are minimized and pore networks are effectively sealed, preventing excessive water ingress and associated swelling. This refined pore structure likewise contributes to improved particle interlocking and a more efficient transfer of loads through the modified soil matrix. Conversely, higher stabilizer concentrations may yield a form of "saturation" effect in which additional binder cannot interact uniformly with soil particles, limiting further gains in microstructural refinement. Consequently, the enhanced cohesion and reduced porosity observed in intermediate-dosage binary systems correlate strongly with both the notable increases in UCS and the mitigated swelling behavior, ultimately confirming that these formulations strike a more favorable balance between cost-effectiveness and long-term performance in expansive soil stabilization.

4 Discussion on the mechanisms of CKD-CCS in soil stabilization

The binary stabilizer system comprising cement kiln dust (CKD) and calcium carbide slag (CCS) demonstrates superior modification efficacy through synergistic physicochemical mechanisms (as shown in Figure 12) in expansive soil matrices. The primary modification mechanism encompasses concurrent physical densification and chemical transformation processes, wherein fine-grained CKD particles facilitate optimal void space occupation while CCS components establish conducive alkaline conditions for secondary pozzolanic reactions. This dual-mechanism approach manifests in systematic enhancement of matrix properties, evidenced by elevated maximum dry density (1.64 g/cm^3 in BSS-10/6) and accelerated strength development (226.3 kPa at 7-day curing in BSS-10/9). Comparative analysis with conventional stabilizers reveals distinctive advantages: the rapid dissolution of CCS-derived CaO establishes immediate strength development through C-A-H formation, demonstrating superior early-stage performance compared to traditional lime stabilization, while the progressive generation of C-S-H gel structures through CKD components facilitates sustained strength enhancement, achieving optimal parameters (371.3 kPa) at 28-day curing. This synergistic interaction, quantified by elevated Synergistic Enhancement Factor (1.65), significantly exceeds the combined individual effects of constituent stabilizers and traditional pozzolanic materials.

The microstructural evolution in CKD-CCS modified matrices provides fundamental validation for the observed macroscopic performance enhancement while demonstrating significant environmental and economic advantages. The progressive development of cementitious compounds facilitates systematic reduction in expansion characteristics, achieving minimal free swelling rate (22.7%) at 28-day maturation in BSS-10/9 configurations - a marked improvement over conventional lime stabilization methodologies. The comprehensive particle encapsulation and enhanced matrix densification manifest in superior durability characteristics, evidenced by sustained strength development during extended curing periods. This represents particular advantages over single-component stabilizers, wherein limited modification mechanisms often result in incomplete matrix transformation. Furthermore, as industrial by-products, both CKD and CCS represent cost-effective alternatives to traditional stabilizers while simultaneously facilitating productive utilization of waste materials. The demonstrated performance characteristics, coupled with these sustainability advantages, establish CKD-CCS stabilization as an optimal methodology for expansive soil modification in practical engineering applications, achieving superior technical performance while advancing sustainable construction practices.

5 Conclusion

This study systematically examined the feasibility of using cement kiln dust (CKD) and calcium carbide slag (CCS) as stabilizers for expansive soil, focusing on compaction characteristics, swelling behavior, unconfined compressive strength (UCS), and microstructural evolution. Based on the experimental findings and analyses, several key conclusions can be drawn:

(1) Compared with the control group (MDD = 1.55 g/cm^3), binary CKD–CCS blends produced higher maximum dry density. BSS-10/6 attained 1.64 g/cm^3. The addition of CKD and CCS reduced the optimal moisture content by occupying soil pores and facilitating early-stage hydration reactions.

(2) Binary stabilizers suppressed volumetric expansion relative to untreated soil. BSS-10/9 decreased the free swelling rate to 22.7% at 28 days. Higher CCS contents (9%–12%) combined with moderate CKD levels led to greater swelling reduction than single-stabilizer systems.

(3) Unconfined compressive strength (UCS) tests indicated substantial gains under CKD–CCS stabilization. BSS-10/9 achieved 226.3 kPa at 7 days and 371.3 kPa at 28 days. The Synergistic Enhancement Factor (SEF) for certain binary formulations exceeded 1.5, indicating that CKD and CCS together outperform individual stabilizers.

(4) SEM analysis confirms CKD–CCS synergy in expansive soils, as hydration products (C-S-H, C-A-H) fill voids and strengthen particle bonds. Moderate dosages optimize pozzolanic reactions for higher density and reduced swelling, whereas excessive content yields diminishing returns due to uneven binder distribution.

(5)BSS-10/9 demonstrated a balanced improvement in densification, swelling control, and UCS, highlighting the low-carbon, cost-effective potential of CKD–CCS blends for stabilizing expansive soil.

Data availability statement

The original contributions presented in the study are included in the article/supplementary material, further inquiries can be directed to the corresponding author.

Author contributions

QY: Conceptualization, Writing–review and editing, Formal Analysis, Funding acquisition, Writing–original draft. BP: Funding acquisition, Writing–original draft, Writing–review and editing, Investigation, Project administration, Validation, Visualization. WL: Project administration, Writing–review and editing, Conceptualization, Resources. BW: Supervision, Writing–review and editing. JZ: Data curation, Visualization, Writing–review and editing. GL: Project administration, Writing–review and editing. TW: Data curation, Writing–review and editing.

Funding

The author(s) declare that financial support was received for the research, authorship, and/or publication of this article. This work was supported by Science and Technology Project of Natural Resources Department of Gansu Province (Major Project, 24JRRA800), 2024 Jiangsu Province construction system research project (2024ZD052), and Xizang Civil water Conservancy and electric power Engineering Technology Research center open project (XZA202405CHP2008B).

Conflict of interest

Author WL was a postdoctoral fellow at Jiangsu Hanjian Group Co., Ltd. Author TW was employed by Jiangsu Hehai Engineering Technology Co., Ltd.

The remaining authors declare that the research was conducted in the absence of any commercial or financial relationships that could be construed as a potential conflict of interest.

Generative AI statement

The author(s) declare that no Generative AI was used in the creation of this manuscript.

Publisher's note

References

Abbas, M. F., Shaker, A. A., and Al-Shamrani, M. A. (2023). Hydraulic and volume change behaviors of compacted highly expansive soil under cyclic wetting and drying. *J. Rock Mech. Geotechnical Eng.* 15 (2), 486–499. doi:10.1016/j.jrmge.2022.05.015

Al-Adhadh, A. R., Daud, N. N. N., Yusuf, B., and Al-Rkaby, A. H. (2024). Supplementary cementitious materials in sandy soil improvement: a review. *J. Build. Pathology Rehabilitation* 9 (2), 138. doi:10.1007/s41024-024-00496-2

Al-Bakri, A. Y., Ahmed, H. M., and Hefni, M. A. (2022). Cement Kiln Dust (CKD): potential beneficial applications and eco-sustainable solutions. *Sustainability* 14 (12), 7022. doi:10.3390/su14127022

Almuaythir, S., and Abbas, M. F. (2023). Expansive soil remediation using cement kiln dust as stabilizer. *Case Stud. Constr. Mater.* 18, e01983. doi:10.1016/j.cscm.2023.e01983

Al-Saedi, M., and Sabbar, A. S. (2024). Treatment of expansive soils with slag: a review study. *Soil Mech. Found. Eng.* 60 (6), 574–580. doi:10.1007/s11204-024-09931-5

Attah, I. C., Okafor, F. O., and Ugwu, O. O. (2021). Optimization of California bearing ratio of tropical black clay soil treated with cement kiln dust and metakaolin blend. *Int. J. Pavement Res. Technol.* 14, 655–667. doi:10.1007/s42947-020-0003-6

Barman, D., and Dash, S. K. (2022). Stabilization of expansive soils using chemical additives: a review. *J. Rock Mech. Geotechnical Eng.* 14 (4), 1319–1342. doi:10.1016/j.jrmge.2022.02.011

Chen, R., Congress, S. S. C., Cai, G., Duan, W., and Liu, S. (2021). Sustainable utilization of biomass waste-rice husk ash as a new solidified material of soil in geotechnical engineering: a review. *Constr. Build. Mater.* 292, 123219. doi:10.1016/j.conbuildmat.2021.123219

Chen, Y., Huang, Y., Wu, M., and Wang, S. (2022). Fly ash/paraffin composite phase change material used to treat thermal and mechanical properties of expansive soil in cold regions. *J. Renew. Mater.* 10 (4), 1153–1173. doi:10.32604/jrm.2022.018856

Chu, C., Zhan, M., Feng, Q., Deng, Y., Li, D., Zha, F., et al. (2023). Expansive soil modified by iron tailing sand and calcium carbide slag as subgrade material. *Environ. Dev. Sustain.* 25 (9), 10393–10410. doi:10.1007/s10668-022-02498-x

Dang, L. C., Khabbaz, H., and Ni, B. J. (2021). Improving engineering characteristics of expansive soils using industry waste as a sustainable application for reuse of bagasse ash. *Transp. Geotech.* 31, 100637. doi:10.1016/j.trgeo.2021.100637

Fatima, B., Alshameri, B., Hassan, W., Maqsood, Z., Jamil, S. M., and Madun, A. (2023). Sustainable incorporation of Plaster of Paris kiln dust for stabilization of dispersive soil: a potential solution for construction industry. *Constr. Build. Mater.* 397, 132459. doi:10.1016/j.conbuildmat.2023.132459

Gong, X., Zhang, T., Zhang, J., Wang, Z., Liu, J., Cao, J., et al. (2022). Recycling and utilization of calcium carbide slag-current status and new opportunities. *Renew. Sustain. Energy Rev.* 159, 112133. doi:10.1016/j.rser.2022.112133

Habert, G., Miller, S. A., John, V. M., Provis, J. L., Favier, A., Horvath, A., et al. (2020). Environmental impacts and decarbonization strategies in the cement and concrete industries. *Nat. Rev. Earth and Environ.* 1 (11), 559–573. doi:10.1038/s43017-020-0093-3

Hassan, W., Alshameri, B., Jamil, S. M., Maqsood, Z., Haider, A., and Shahzad, A. (2023). Incorporating potassium-rich waste material in a sustainable way to stabilize dispersive clay: a novel practical approach for the construction industry. *Constr. Build. Mater.* 400, 132717. doi:10.1016/j.conbuildmat.2023.132717

Laporte, S., Eichhorn, G., Kingswood, J., Siemens, G., and Beddoe, R. (2023). Physical modelling of climate-soil-infrastructure interactions of paved roadways constructed in expansive soil. *Transp. Geotech.* 43, 101126. doi:10.1016/j.trgeo.2023.101126

Liu, Z., Ma, X., Chi, J., Chen, Y., and Wang, C. (2024). Centrifuge model tests and numerical simulation on ground-borne vibration propagating and vibration reduction scheme for tunnel inner structure. *Tunn. Undergr. Space Technol. incorporating Trenchless Technol. Res.* 153, 105996. doi:10.1016/j.tust.2024.105996

Mahedi, M., Cetin, B., and White, D. J. (2020). Cement, lime, and fly ashes in stabilizing expansive soils: performance evaluation and comparison. *J. Mater. Civ. Eng.* 32 (7), 04020177. doi:10.1061/(asce)mt.1943-5533.0003260

Ministry of Construction P.R.China (2019). *GB/T 50123-2019 Standard for soil test method*. Beijing: China Planning Press.

Ministry of Transport P.R. China (2007). *JTG E40-2007 Test methods of soils for highway engineering*. Beijing: China communication press.

Miraki, H., Shariatmadari, N., Ghadir, P., Jahandari, S., Tao, Z., and Siddique, R. (2022). Clayey soil stabilization using alkali-activated volcanic ash and slag. *J. Rock Mech. Geotechnical Eng.* 14 (2), 576–591. doi:10.1016/j.jrmge.2021.08.012

Mustafayeva, A., Moon, S.-W., Satyanaga, A., and Kim, J. (2024). Enhancing mechanical properties of expansive soil through BOF slag stabilization: a sustainable alternative to conventional methods. *Minerals* 14, 1145. doi:10.3390/min14111145

Muthukkumaran, K., and Anusudha, V. (2020). Study on behavior of copper slag and lime–treated clay under static and dynamic loading. *J. Mater. Civ. Eng.* 32 (8), 04020230. doi:10.1061/(asce)mt.1943-5533.0003259

Sarker, D., Apu, O. S., Kumar, N., Wang, J. X., and Lynam, J. G. (2023). Sustainable lignin to enhance engineering properties of unsaturated expansive subgrade soils. *J. Mater. Civ. Eng.* 35 (8), 04023259. doi:10.1061/jmcee7.mteng-15008

Shan, Y., Huang, A., Qin, X., Zhou, S., and Zhou, X. (2022). Long-term *in-situ* monitoring on foundation settlement and service performance of a novel pile-plank-supported ballastless tram track in soft soil regions. *Transp. Geotech.* 36, 100821. doi:10.1016/j.trgeo.2022.100821

Song, J., Lu, Z., Pan, Y., Ji, J., and Gao, Y. (2024). Investigation of seismic displacements in bedding rock slopes by an extended Newmark sliding block model. *Landslides* 21 (3), 461–477. doi:10.1007/s10346-023-02170-z

Syed, M., GuhaRay, A., and Goel, D. (2022). Strength characterisation of fiber reinforced expansive subgrade soil stabilized with alkali activated binder. *Road Mater. Pavement Des.* 23 (5), 1037–1060. doi:10.1080/14680629.2020.1869062

Syed, M., GuhaRay, A., and Raju, S. (2023). Subgrade strength performance behavior of alkali-activated binder and cement stabilized expansive soil: a semifield study. *J. Mater. Civ. Eng.* 35 (10), 04023329. doi:10.1061/jmcee7.mteng-15580

Tiwari, N., Satyam, N., and Puppala, A. J. (2021). Strength and durability assessment of expansive soil stabilized with recycled ash and natural fibers. *Transp. Geotech.* 29, 100556. doi:10.1016/j.trgeo.2021.100556

Wang, H., Jiang, M., Cao, B., Wang, F., and Xu, J. (2024). Stabilized/solidified chlorine saline soils with ground granulated blast furnace slag and calcium carbide residue. *Constr. Build. Mater.* 449, 138490. doi:10.1016/j.conbuildmat.2024.138490

Wei, J., Wei, J., Huang, Q., Zainal Abidin, S. M. I. B. S., and Zou, Z. (2023). Mechanism and engineering characteristics of expansive soil reinforced by industrial solid waste: a review. *Buildings* 13 (4), 1001. doi:10.3390/buildings13041001

Wu, Y., Qiao, X., Yu, X., Yu, J., and Deng, Y. (2021). Study on properties of expansive soil improved by steel slag powder and cement under freeze-thaw cycles. *KSCE J. Civ. Eng.* 25 (2), 417–428. doi:10.1007/s12205-020-0341-6

Ye, W., Gao, C., Liu, Z., Wang, Q., and Su, W. (2023). A Fuzzy-AHP-based variable weight safety evaluation model for expansive soil slope. *Nat. Hazards* 119 (1), 559–581. doi:10.1007/s11069-023-06130-7

Zada, U., Jamal, A., Iqbal, M., Eldin, S. M., Almoshaogeh, M., Bekkouche, S. R., et al. (2023). Recent advances in expansive soil stabilization using admixtures: current challenges and opportunities. *Case Stud. Constr. Mater.* 18, e01985. doi:10.1016/j.cscm.2023.e01985

Zhang, C., Wang, W., Zhu, Z., Shao, L., Wan, Y., and Zhang, Y. (2023). Mechanical and microscopic properties of cement composite expansive soil with graphene oxide: ecofriendly modification material. *Int. J. Geomechanics* 23 (6), 04023071. doi:10.1061/ijgnai.gmeng-8574

Zhao, G., Yan, D., Ren, G., Zhu, Z., Wu, T., Ding, S., et al. (2023). Influence of ground granulated blast furnace slag on the dispersivity and mechanical property of dispersive soil. *Constr. Build. Mater.* 409, 134036. doi:10.1016/j.conbuildmat.2023.134036

Zheng, X., Liu, K., Gao, S., Wang, F., and Wu, Z. (2023). Effect of pozzolanic reaction of zeolite on its internal curing performance in cement-based materials. *J. Build. Eng.* 63, 105503. doi:10.1016/j.jobe.2022.105503